



Cite this: *Sustainable Energy Fuels*, 2022, **6**, 2823

Technoeconomic analysis of corn stover conversion by decentralized pyrolysis and electrocatalysis†

Sabyasachi Das, ^a James E. Anderson, ^b Robert De Kleine, ^b Timothy J. Wallington, ^b James E. Jackson ^c and Christopher M. Saffron ^{*ad}

Maximizing fossil fuel displacement and limiting atmospheric carbon dioxide levels require a high efficiency of carbon incorporation in bioenergy systems. The availability of biomass carbon is a constraint globally, and strategies to increase the efficiency of bioenergy production and biogenic carbon use are needed. Previous studies have shown that "energy upgrading" of biomass by coupling with renewable electricity through electrocatalytic hydrogenation offers a potential pathway to near full petroleum fuel displacement in the U.S., even when annual U.S. biomass production is limited to 1.2 billion dry tonnes. Commercialization of such technology requires economic feasibility. A technoeconomic model of decentralized, depot-based pyrolysis with electrocatalytic hydrogenation and centralized upgrading (Py-ECH), producing liquid hydrocarbon fuel is presented and compared to a cellulosic ethanol pathway using consistent assumptions. Using a discounted cash flow approach, a minimum fuel selling price (MFSP) of \$3.62 per gallon gasoline equivalent (GGE) or \$0.96 per gasoline liter equivalent (GLE) is estimated for Py-ECH fuel derived from corn stover, considering n^{th} plant economics and a fixed internal rate of return of 10%. This is comparable to the MFSP for cellulosic ethanol from fermentation with the same feedstock (\$3.71 per GGE or \$0.98 per GLE) and is in the range of gasoline prices over the last 20 years of \$1 per GGE (\$0.26 per GLE) to \$4.44 per GGE (\$1.17 per GLE) in 2018. Optimization studies on depot sizing identified a trade-off between transportation and economies-of-scale costs, with an optimum size of 500 tpd. Sensitivity analyses showed that electricity cost, raw material costs, bio-oil yields, and cell efficiencies are the key parameters that affect the Py-ECH MFSP. With system improvements, a pathway to less than \$3 per GGE or \$0.79 per GLE is articulated for liquid hydrocarbon fuel from corn stover using Py-ECH.

Received 25th November 2021
Accepted 24th April 2022

DOI: 10.1039/d1se01881g
rsc.li/sustainable-energy

1. Introduction

The U.S. Department of Energy's "2016 Billion-Ton Report" projected the total harvestable biomass available in the U.S. to be 1.3 billion dry tons by the year 2030 for biomass obtained at a cost of less than \$60 per dry ton. While this is a large quantity, the carbon and energy content of this biomass is insufficient to meet the energy demands of the U.S. transportation sector. It is important to develop bioenergy systems that utilize renewable energy and carbon efficiently. Py-ECH has an advantage over cellulosic ethanol in terms of carbon efficiency, as one-third of the holocellulosic carbon is lost as carbon dioxide during

fermentation.¹ Moreover, combusting lignin for internal heat and power also diverts carbon away from incorporation into higher-value liquid fuels.

Nearly all liquid biofuel strategies require biomass deconstruction as an early step in processing. The literature on deconstruction is immense and growing, as new techniques involving acids, bases, solvents, enzymes, heat, and combinations thereof continue to emerge. Of the many existing deconstruction techniques, biomass fast pyrolysis is well-studied and can be achieved with low capital cost and high yield because of short residence times. Further, it converts a portion of the biomass lignin along with the holocellulose into the primary product, bio-oil.¹⁻³ Regional biomass processing depots to produce bio-oil are capable of lowering overall hauling costs because bulk density is increased,⁴ however the reactivity of bio-oil limits its ability to be transported. Functional groups such as carbonyls, carboxylates, and alcohols react to form polymers which increase viscosity and form sludges. Further, bio-oil from pyrolysis is corrosive to metals as it contains weak acids and has high total acid number (TAN).

^aDepartment of Chemical Engineering and Materials Science, Michigan State University, East Lansing, Michigan, 48824, USA. E-mail: saffronc@msu.edu

^bResearch and Advanced Engineering, Ford Motor Company, Dearborn, MI 48121, USA

^cDepartment of Chemistry, Michigan State University, East Lansing, MI 48824, USA

[†]Department of Biosystems and Agricultural Engineering, Michigan State University, East Lansing, MI 48824, USA

† Electronic supplementary information (ESI) available. See <https://doi.org/10.1039/d1se01881g>

Bio-oil is unsuitable for transport and storage and needs to be stabilized immediately after pyrolysis. Thermal hydrogenation and hydrodeoxygenation have been used for hydrogenating and stabilizing bio-oil,^{3,5–16} however, these techniques operate under high temperature and pressure and are not suited for widespread deployment in small-scale plants (depots).⁴ A milder alternative is electrocatalytic hydrogenation (ECH), which involves the electrolysis of water to produce *in situ* hydrogen ions on the anode that electrocatalytically react with bio-oil on the cathode. This technique has been shown to successfully hydrogenate and deoxygenate the variety of compounds found in raw biomass-derived bio-oil as well as lignin-derived bio-oil.^{17–23} ECH is a promising strategy because it operates at mild conditions, avoids storage or use of hydrogen gas, and also reduces hydrogen consumption at the centralized refinery where hydroprocessing can be safely utilized to create finished fuels.^{17,19} Sequential fast pyrolysis and electrocatalysis (Py-ECH) co-deployed in a biomass upgrading depot, followed by petroleum-style hydroprocessing in central refineries, potentially offers a carbon and energy efficient strategy for making liquid hydrocarbon biofuels.¹

While such a decentralized biorefinery system shows promise in terms of carbon and energy efficiency, its economics must be investigated. Technoeconomic analyses have been completed for centralized pyrolysis followed by hydroprocessing. Wright²⁴ *et al.* estimated a minimum fuel selling price (MFSP) of \$2.41 per GGE (\$0.64 per GLE) when the merchant H₂ is purchased at \$1.47 per kg H₂ for hydroprocessing. (All costs herein are determined or converted to 2018\$.) However, when a portion of the bio-oil is steam reformed to make the H₂ gas required for upgrading the remaining bio-oil, the MFSP of the fuel increased to \$3.55 per GGE (\$0.94 per GLE). Brown *et al.*²⁵ estimated an MFSP of \$2.64 per GGE (\$0.70 per GLE) for a pyrolysis and hydroprocessing facility that processed 2000 tonnes per day (tpd) of corn stover. Jones *et al.*²⁶ estimated the MFSP of a hydrocarbon fuel derived from pyrolysis and hydrotreating of hybrid poplar to be \$2.34 per GGE (\$0.2 per GLE). Dutta *et al.*²⁷ determined the MFSP of hydrocarbon fuel produced from the pyrolysis and vapor upgrading of lignocellulosic biomass to be in the range of \$3.41 per GGE (\$0.9 per GLE) to \$3.56 per GGE (\$0.95 per GLE), depending on whether the upgrading is done *in situ* or *ex situ*. Carrasco *et al.*²⁸ estimated the economics for pyrolysis and hydrotreating of forest residues to make liquid fuels and found an MFSP of \$6.64 per GGE (\$1.75 per GLE). These MFSPs fall in the range of \$2.17–7.24 per GGE (\$0.54–1.8 per GLE) reported by Sorunmu *et al.*²⁹ in their review of technoeconomic analyses for the pyrolysis and upgrading of lignocellulosic biomass. None of these systems, however, considered decentralized upgrading or the use of ECH.

Orella *et al.*³⁰ investigated the technoeconomics of the ECH process alone and developed a model to estimate the MFSP of reducing guaiacol, a pyrolysis bio-oil representative compound, to phenol. It was reported that with enhanced current density, decreased selectivity for hydrogen evolution and increased faradaic efficiencies for the desired product, the selling price for phenol can drop from \$28.67 per kg to \$0.42 per kg.

In the present work, a technoeconomic analysis has been performed for the full-scale combined Py-ECH process that

upgrades biomass (corn stover) to a stable fuel intermediate in decentralized depots, which is then delivered to a centralized refinery that uses traditional hydroprocessing to produce a liquid hydrocarbon fuel. The produced liquid hydrocarbon fuel mixture is assumed to have properties of iso-octane, representative of gasoline. This liquid hydrocarbon fuel is the major component of the refinery's finished fuel output. Sensitivity analyses were conducted to identify key parameters that influence the MFSP, with the objective of guiding researchers towards economically relevant process improvements. Unless specified otherwise, all costs are in 2018\$.

2. Materials and methods

2.1. Process description

The process under investigation combines fast pyrolysis of corn stover and subsequent electrocatalytic hydrogenation (Py-ECH) in depots with hydroprocessing in a central refinery to produce liquid fuels from biomass (Fig. 1) as described in detail elsewhere.³¹ In brief, the Py-ECH system involves hauling biomass from the cultivation fields to regional depots where it is ground and dried prior to deconstruction in a fast pyrolysis reactor at 500 °C and atmospheric pressure. The assumed mass percentages of the pyrolysis products are 70%, 15%, and 15% for liquid bio-oil, biochar, and non-condensable gases, respectively. The resultant bio-oil is then electrocatalytically reduced in an ECH unit at 80 °C and atmospheric pressure. Ruthenium metal serves as the electrocatalyst. ECH-stabilized bio-oil is then transported to a central hydroprocessing facility where it is further upgraded to liquid hydrocarbon fuel using hydrogen at 400 °C and 200 bar pressure in the presence of Co–Mo catalyst.³² The hydrogen is assumed to be renewably generated by electrolysis of water at the central refinery.

Economics of cellulosic ethanol produced *via* fermentation of corn stover feedstock were evaluated using the analysis by Humbird *et al.*³³ at the National Renewable Energy Laboratory (NREL). The analysis was used as a framework for the Py-ECH analysis, using the same assumptions where possible and appropriate, including a 2000 tonne per day biomass processing scale as the combined input to the system of Py-ECH depots. Multiple depots, equally sized, supply a single centralized refinery to make the finished hydrocarbon fuel component. Depot sizes in previous literature have varied, for example Eranki *et al.* reported values of 100 tpd⁴ and Lamers *et al.* assumed a maximum of 215 tpd.³⁴ The depot size in the present analysis was fixed after an optimization study that minimized the total system transportation cost, from fields to depots to central refinery. The assumed composition and moisture content of the delivered corn stover at the depot gate were the same as the Humbird *et al.* report.³³ Material and energy balances required for the Py-ECH and cellulosic ethanol economics were extracted from our previous work³¹ and the NREL study, respectively.

2.2. Economic model

The economic modeling and assumptions for the Py-ECH system were consistent with that for an *n*th plant in the

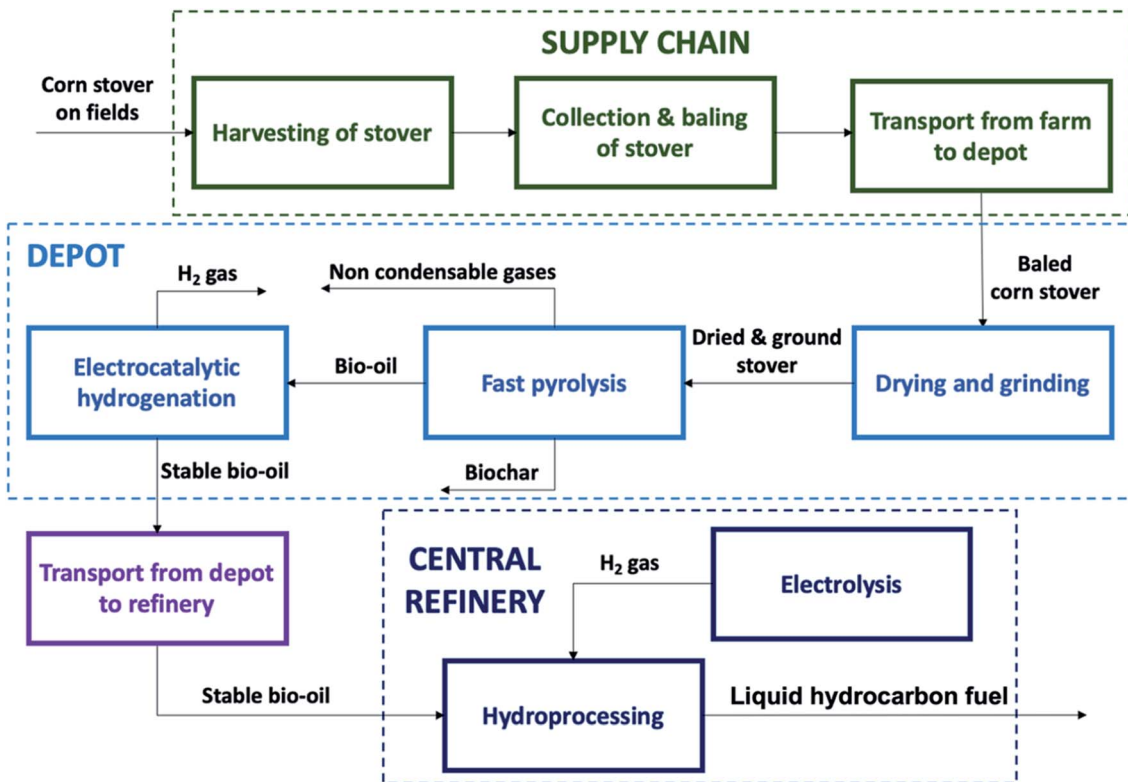


Fig. 1 Py-ECH process flow diagram with pyrolysis and electrocatalytic hydrogenation in decentralized depots and hydroprocessing in centralized refineries.

Table 1 Assumptions in the technoeconomic model

Parameter	Value
Plant life	30 years
Plant location	Midwest USA
Cost basis year	2018
Internal rate of return	10%
Depreciation method	200% double declining balance
Federal tax rate	35%
Working capital	5% of fixed capital investment
Salvage value	0\$
Construction period	1 year
Startup period	3 months
Revenues during startup	50%
Variable costs during startup	75%
Fixed costs during startup	100%
Loan terms	8% APR; 10 years
Financing	40% equity

Humbird *et al.* report for ethanol production *via* fermentation of cellulose.³³ The minimum fuel selling price (MFSP) of the fuel produced was determined using a discounted cash flow analysis (DCFA) with a fixed internal rate of return. This was performed by iterating the MFSP until the net present value of all cash flows for the entire plant life equaled zero. It must be noted that the DCFA was performed twice, first at the depot, and then at the central refinery. For the depot, the raw material was the corn stover biomass and the finished product was the ECH-stabilized bio-oil. For the central refinery, the raw material was this ECH-

stabilized bio-oil and the product was isooctane, the final hydrocarbon fuel component.

Economic assumptions for the technoeconomic modeling are summarized in Table 1. The total capital investment included fixed capital investment (FCI), land, and working capital (assumed 5% of FCI). The FCI, in turn, included both direct and indirect costs and were functions of the total installed equipment costs. Installed equipment costs were determined by applying an installation multiplier to the estimated equipment cost. Details behind these equipment costs are described in the ESI† and a data inventory is given in Table S5.† Operating costs were determined by summing the fixed costs (e.g., employee salaries, insurance, and maintenance costs) and variable costs (e.g., raw materials and utilities). While the fixed operating costs were percentages of the total capital investment, the variable operating costs were either estimated from literature data or calculated. For instance, the raw material cost for the Py-ECH system was estimated from a supply chain analysis, described in the next section.

2.2.1. By-products. In addition to the ECH bio-oil, the Py-ECH system generates two by-products at the depot: biochar and H₂ from the ECH unit. While the biochar is not utilized in the process, some of the ECH H₂ is utilized, in combination with the non-condensable gases from the pyrolyzer, to meet the heat requirements at the depot. Excess H₂ and biochar may be sold for additional revenue to bring down the cost of the final Py-ECH fuel. This is similar to the approach adopted in the NREL cellulosic ethanol study in which revenue from selling

excess electricity was incorporated to determine the final MFSP of the fuel. The H₂ price was fixed at \$2 per kg, which is the U.S. Department of Energy 2020 total leveled cost target for generation from electrolysis.³⁵ This falls within the range for the cost of H₂ generated from steam reforming, from \$1.25 per kg for large systems to \$3.50 per kg for smaller systems.³⁶ There is a large range of estimated selling prices for biochar in the literature. Campbell *et al.* reviewed different biochar production scenarios and estimated selling prices from \$80 per tonne to about \$13 000 per tonne in 2013.³⁷ The selling price of biochar depends heavily on its quality as determined by its carbon and ash contents, the biomass source, and whether it is a wholesale or retail price, among other factors.³⁷ Table S2 in the ESI† provides a range of biochar prices from the literature. Due to the high uncertainty in the value and quality of the biochar being generated, the baseline scenario of the present study assumes that biochar has no value and is not sold. A sensitivity analysis was conducted in which biochar was assigned a conservative value.

2.3. Supply chain

The price of delivered corn stover for cellulosic fermentation to ethanol (CE) was taken from the Humbird *et al.* report and adjusted to 2018\$ using Chemical Engineering Plant Cost Indices.³⁸ Costs were originally estimated from the Department of Energy's Multi-Year Program Plan (MYPP) published in 2011. While the 2016 MYPP has since been published, we employed values from the 2011 report as the 2016 MYPP mostly explores blended feedstock with less focus on corn stover as the sole feedstock. The major components of the feedstock price are harvesting and collection, feedstock storage, preprocessing, transportation and handling, and the grower payment. To maintain consistency, the same assumptions were used for the Py-ECH system with a few exceptions. The preprocessing costs involved drying and grinding operations, aimed at making the

raw material fit for processing. These costs are included as separate unit operations at the depot and therefore excluded from the raw material cost for the Py-ECH system.

Another key difference between the two systems is logistics. While all corn stover is directly brought to a single cellulosic ethanol biorefinery in the CE system, transportation in the Py-ECH system occurs in two stages. Corn stover is first transported over short distances from fields to depots, and later the stable bio-oil is transported from the depots to the central refinery. To estimate the transportation cost of delivering raw corn stover to depots in the Py-ECH system, we conducted an optimization study to minimize the minimum fuel selling price (MFSP). Kim and Dale³⁹ reported an equation giving optimal depot size based on farm-to-depot transportation distance (see Tables S3 and S4† of ESI†). Kim and Dale assumed a solar-system-like model, where the refinery is located at the center, with all the depots located in rings around the refinery and with each depot having its own collection radius.

In the present analysis, a square geometry was assumed (as land is commonly parceled). Fig. 2(a) shows one instance of an example configuration. The central refinery (red square) is located in the center, while the depots (black stars) are scattered around the refinery. The green squares represent the biomass collection area for the depot located at its center and are assumed to constitute 25% of the land area.⁴⁰ The white spaces denote the 75% not dedicated to crop cultivation. No depots were assumed to be located in the region adjacent to the refinery, denoted by the blue boundary, to avoid a situation where the biomass is closer to the refinery than the depot. The depot arrangement shown in Fig. 2(a) is one of many arrangements, each with different average depot-to-refinery distance and consequently, different transportation costs. Therefore, optimization was performed for determining the optimal placement of the depots around the central refinery that resulted in the lowest total transportation cost. Fig. 2 (b) shows how

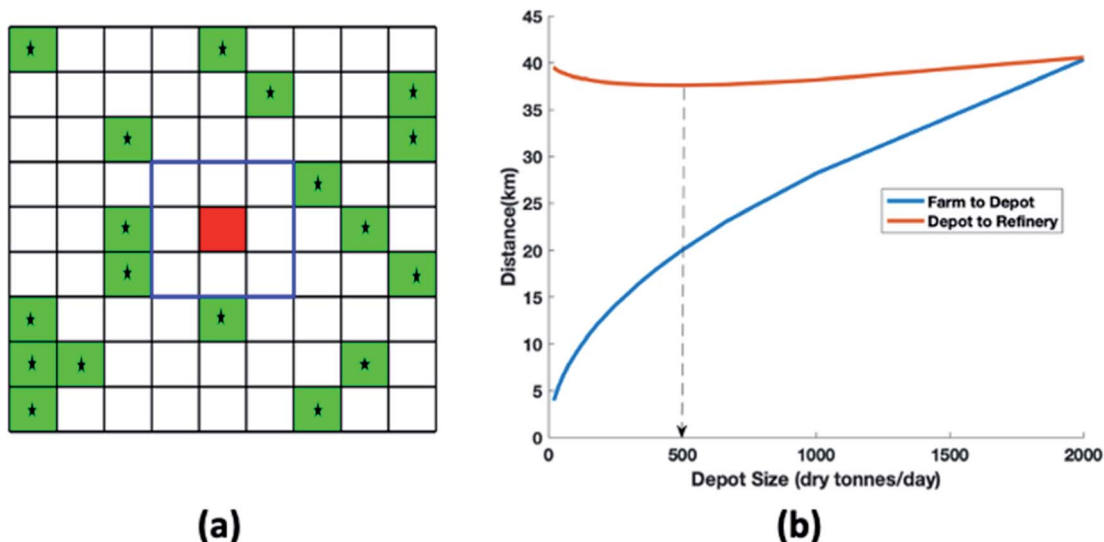


Fig. 2 (a) Illustration of a random depot distribution (black stars) and their biomass collection areas (green squares) relative to central refinery (red square), for a central refinery with 18 depots. (b) Farm-to-depot and depot-to-refinery distance versus depot size for a 2000 tpd central refinery.

the depot-to-refinery distance, and the farm-to-depot distance varies with depot size for a 2000 tonne per day central refinery. Further details are given in the ESI.†

The farm-to-depot distance varies as the square root of the depot size as the land has been parcelled into squares. The depot-to-refinery distance goes through a slight minimum at a depot size of 500 tpd but does not vary greatly for higher and lower sizes because the depots are fairly close together when the central refinery size is 2000 tpd.

3. Results

3.1. Supply chain costs

Using the optimization strategy and the economic model outlined in the previous sections, the minimum fuel selling price (MFSP) was calculated for different depot and refinery sizes

(Fig. 3). For all refinery sizes (except for a 1000 tpd central refinery), the MFSP passes through a minimum as depot sizes are increased. As depot size increases, the MFSP initially decreases reflecting economies-of-scale. For still larger depot sizes, longer field-to-depot distances overwhelm the economies-of-scale benefit. The minimum transportation cost occurs for depot sizes of 500–1000 tpd, as highlighted in Fig. 3 by dotted vertical lines. For a 1000 tpd central refinery, a minimum was not observed as transportation distances are not large enough to overcome the improving economies-of-scale. It must be noted here that the sharp changes in slope observed in the profile for some of the refinery sizes (e.g., for $C_R = 10\,000$ tpd) is due to the fact that the MFSP is not a continuous function of the depot size. Furthermore, the change in depot size is sometimes not large enough to effect an observable change in the MFSP. For the present analysis which assumes a refinery capacity of 2000

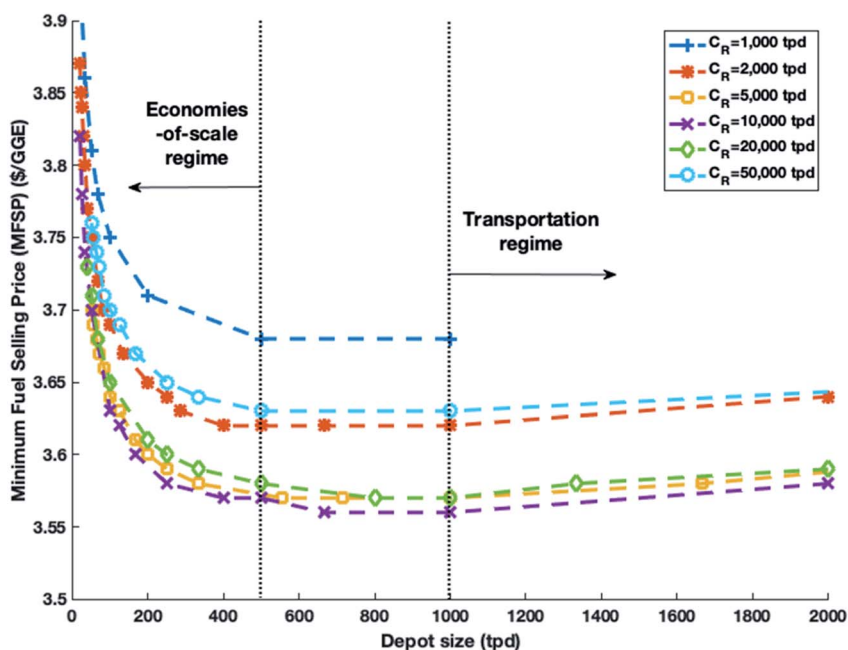


Fig. 3 MFSP versus depot size for different central refinery processing capacities, C_R .

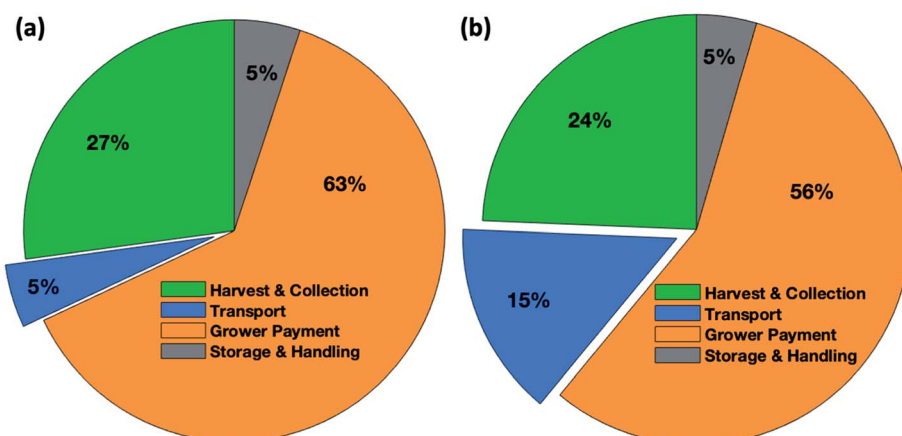


Fig. 4 Raw material supply chain costs from farm to depot gate for Py-ECH (a) and from farm to refinery for CE system (b).

tpd, the minimum was observed for a depot size of 500 tpd, *i.e.*, 4 depots per refinery. This value is consistent with the minimum depot-to-refinery travel distance seen in Fig. 2(b).

Next, the costs of transporting biomass from farm-to-depot and transporting the ECH bio-oil from depot-to-refinery were determined. Using the average farm-to-depot (24.7 km) and depot-to-refinery distances (46.3 km) for the optimized depot arrangement with a trucking cost of \$1.82 per mile (in 2018\$)⁴¹ gives a transport cost of \$2.97 per tonne for biomass farm-to-depot delivery and a cost of \$7.71 per tonne of ECH bio-oil delivered from a depot to a refinery. The total transportation cost for the Py-ECH system of \$7.82 per tonne of biomass is lower than the \$10 per tonne of biomass assumed by Humbird *et al.* for the CE system, which highlights the advantage of decentralization to reduce overall transport costs. The use of decentralized Py-ECH is the only difference between the two supply chains; all other costs related to biomass harvesting, collection and storage, and grower payments are the same. The total cost of delivered raw biomass is \$68.33 per tonne of dry biomass for the CE system and \$61.30 per tonne for the Py-ECH system. The relative contributions of different components of the two supply chains are shown in Fig. 4(a) and (b) and the absolute values are reported in Table S4.† The grower payment, which includes the cost of corn stover production and the growers' profit margin, dominate both systems. This is followed by the costs associated with harvesting, baling, and collecting stover. The major difference between the two systems is transportation: 15% of the supply chain costs in the CE system, but only 5% in the Py-ECH system. It must, however, be noted here that this transportation does not include the costs of transporting the ECH bio-oil from the depot to the refinery for the Py-ECH system.

3.2. Depot costs

Table 2 and Fig. 5 show the capital and operating costs at a 500 tpd Py-ECH depot. The total capital investment for a single depot is \$29M, while the annual operating costs are about \$25M. Capital costs at the depot are dominated by the ECH unit (67%) followed by the pyrolysis, combustion, and drying units. This reflects the high cost of the membrane electrode assembly stacks that are made of expensive noble metals (Pt anode and Ru cathode). Combustion, pyrolysis, and drying are the next highest costs, as high-temperature reaction vessels are used. The variable operating costs at the depot include the costs of raw materials, electricity, fresh water for ECH, and ECH stack replacement. Grid electricity (assumed at \$0.0656 per kW per h)³³ is about 63% of operating costs, reflecting the large electric energy requirement of ECH. Raw material costs (36%) are also significant because of the various supply chain costs already described. ECH stack replacement costs, assumed at 15% of the installed capital costs with a replacement schedule of 7 years are negligible (<1%), as seen in Fig. 5(b).

3.3. Refinery costs

Table 3 shows the estimated capital and operating costs at the refinery. The total capital investment for the central refinery is

Table 2 Depot capital and operating costs (500 tpd Depot)

Total capital cost (2018\$)		
Unit	Installed cost	Percentage (%)
Drying	1 240 000	8.3
Grinding	167 000	1.1
Pyrolysis	1 300 000	8.8
Condensation	14 500	0.1
ECH	992 000	66.6
Combustion	1 490 000	10.0
Storage	758 000	5.1
Total installed capital cost	14 900 000	100.0
Inside battery limits capital cost	12 600 000	
Direct costs		
Total installed capital cost	14 900 000	87.1
Warehouse	505 000	3.0
Site development	1 140 000	6.6
Additional piping	569 000	3.3
Total direct costs	17 100 000	100.0
Indirect costs		
Proratable costs	1 710 000	16.7
Field expenses	1 710 000	16.7
Home office and construction	3 420 000	33.3
Project contingency	1 710 000	16.7
Other costs	1 710 000	16.6
Total indirect costs	10 300 000	100.0
Fixed capital investment (FCI)		
Land	238 000	0.8
Working capital	1 370 000	4.7
Total capital investment (TCI)	29 000 000	100.0
Total operating costs (2018\$ per year)		
Variable operating costs		
Raw material	8 840 000	35.8
Grid electricity	15 600 000	63.2
Fresh water	19 700	0.1
ECH stack replacement	212 000	0.9
Total variable operating costs	24 700 000	100.0
Fixed operating costs		
Salaries	145 000	17.1
Labor	130 000	15.4
Maintenance	379 000	44.8
Property insurance	192 000	22.7
Total fixed operating costs	846 000	100.0
Total variable operating costs	24 700 000	96.7
Total fixed operating costs	846 000	3.3
Total operating costs	25 500 000	100.0

\$227M for processing the amount of bio-oil generated from pyrolyzing a total of 2000 tpd of raw biomass from all the depots combined. The annual operating costs are around \$161M.

The refinery electrolyzer costs account for 58% of the total capital, while hydroprocessing comprises most of the remaining 42% as shown in Fig. 6(a). The high costs for the electrolyzer are again attributed to the high cost of the membrane electrode assembly stacks in the electrolyzer.

Table 3 Refinery capital and operating costs (2000 tpd refinery)

Total capital cost (2018\$)		
Unit	Installed cost	Percentage (%)
Hydroprocessing	47 900 000	42.0
Electrolysis	66 000 000	57.8
Storage	210 000	0.2
Total installed capital cost	114 000 000	100.0
Inside battery limits capital cost	114 000 000	
Direct costs		
Total installed capital cost	114 000 000	85.1
Warehouse	4 560 000	3.4
Site development	10 300 000	7.7
Additional piping	5 130 000	3.8
Total direct costs	134 000 000	100.0
Indirect costs		
Proratable costs	13 400 000	16.7
Field expenses	13 400 000	16.7
Home office and construction	26 800 000	33.3
Project contingency	13 400 000	16.7
Other costs	13 400 000	16.6
Total indirect costs	80 400 000	100.0
Fixed capital investment (FCI)	215 000 000	94.47
Land	183 000 000	0.80
Working capital	10 700 000	4.72
Total capital investment (TCI)	227 000 000	100.00
Total operating costs (2018\$ per year)		
Variable operating costs		
Raw material	100 000 000	65.1
Grid electricity	42 700 000	27.6
Natural gas	7 230 000	4.7
Electrolyser stack replacement	1 410 000	0.9
Hydroprocessor catalyst replacement	2 640 000	1.7
Total variable operating costs	154 000 000	100.0
Fixed operating costs		
Salaries	1 140 000	16.1
Labor burden	1 020 000	14.4
Maintenance	3 420 000	48.3
Property insurance	1 500 000	21.2
Total fixed operating costs	7 080 000	100.0
Total variable operating costs	154 000 000	95.6
Total variable operating costs	154 000 000	4.4
Total operating costs	161 000 000	100.0

The refinery variable operating costs in Fig. 6(b) include raw material (stable bio-oil procured from the depots), electricity for the electrolyzer to produce H₂ gas, natural gas for process heating, electrolyser stack replacement, and hydroprocessing catalyst replacement costs. The chief contributor to operating costs (65%) is the raw material purchased from the depots. This is essentially the MFSP (considering an internal rate of return of 10%) of the ECH bio-oil at the depot exit plus the cost of transporting the stable bio-oil from the depot to the refinery (3.4% of the raw material costs). Electricity accounts for 28% of the operating costs at the refinery, natural gas accounts for 5%, and other costs are negligible.

3.4. Minimum fuel selling price

Technoeconomic analysis of the Py-ECH system, using a DCFA approach with an internal rate of return of 10%, yields an MFSP of \$1.17 per GGE (\$0.31 per GLE) for the stable bio-oil produced by the depot and an MFSP of \$3.62 per GGE (\$0.96 per GLE) for the fuel component produced by the refinery. For comparison, the MFSP for cellulosic ethanol was calculated to be \$2.47 per gallon (\$3.71 per GGE or \$0.98 per GLE). Therefore, under the current assumptions, Py-ECH fuel is slightly cheaper than the cellulosic ethanol product on an energy basis. As a hydrocarbon product, the Py-ECH fuel has advantages over ethanol such as higher theoretical blending levels in gasoline or diesel fuel, compatibility with the conventional fuel distribution infrastructure and vehicles, and greater volumetric energy density. The extent to which the Py-ECH-HP hydrocarbons could be blended into gasoline or diesel will depend on its molecular size and structure, which determines its volatility and octane or cetane value.

3.5. Sensitivity analyses

3.5.1. Effect of model parameters. Sensitivity analyses were performed to determine the key parameters affecting the MFSP of the Py-ECH fuel product. Electricity cost, raw material cost, bio-oil yield, internal rate of return (IRR), electrocatalytic cell efficiencies, catalyst price and thickness, costs associated with catalyst replacement, capital costs at depot and refinery, and the selling price of by-product hydrogen were investigated. The values of these parameters were changed by either 50% or 25%, and the results are shown as a tornado chart in Fig. 7. A 25% change was only employed when a 50% change from the baseline value was impractical, *e.g.*, a 50% increase in the assumed 70% bio-oil yield is not possible. Electricity and raw material costs are the most sensitive parameters in determining MFSP. This is intuitive since the Py-ECH system is a major consumer of electricity and raw materials are the other major cost contributor. Bio-oil yield, current and voltage efficiencies, the assumed internal rate of return, and catalyst price and thickness are also important. An increase in bio-oil yield and the cell efficiencies leads to reduced losses in the system and an increase in the overall yield of the final fuel. The ECH catalyst price and thickness are also sensitive parameters. The catalyst replacement costs, whether in the ECH at the depot or the hydroprocessor at the central refinery, are not sensitive parameters because the replacement schedule of the ECH stack requires 15% of the installed capital cost of the stack every seven years. Similarly, the MFSP is relatively insensitive to the capital costs at the depot and refinery. Of the eight most sensitive parameters, five are directly linked to the ECH unit. Of the remaining three, two are related to the pyrolysis unit and one, the IRR, is an economic parameter that impacts all system costs. As both the pyrolysis and ECH units are at the depot, the sensitivity analysis points towards opportunities at the depot for further optimizing the economics of the Py-ECH-HP system. Attention could be focused on optimizing the ECH catalyst, process conditions, and efficiencies in comparison to equipment capital costs.

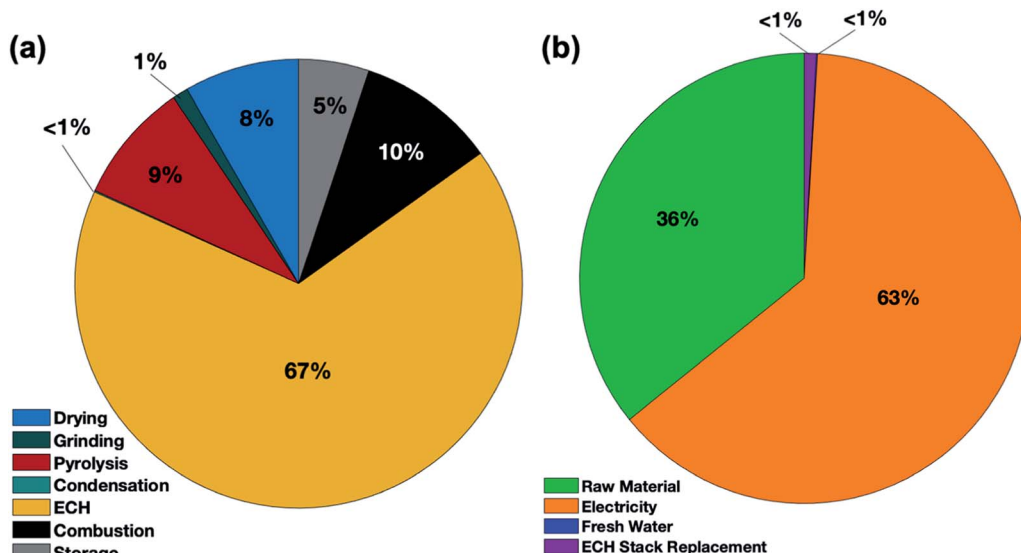


Fig. 5 (a) Capital cost breakdown for a 500 tpd depot (b) variable operating cost breakdown for a 500 tpd depot.

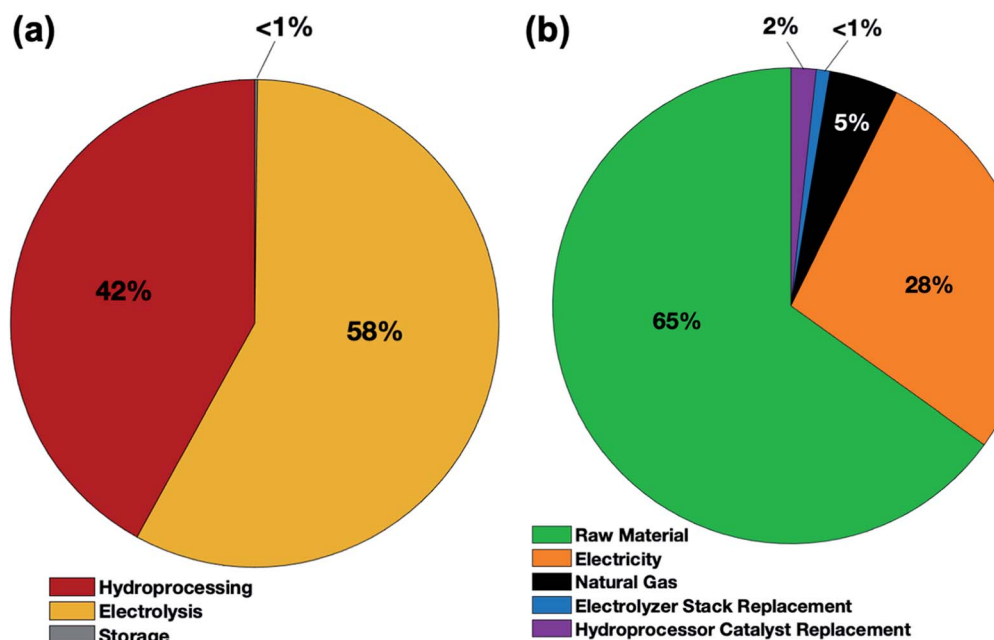


Fig. 6 Refinery capital (a) and variable operating cost (b) breakdown.

3.5.2. Effect of refinery size. Consistent with the Humbird *et al.* cellulosic ethanol process analysis, the baseline refinery size was assumed to be 2000 tpd. Additionally, variation of MFSP with refinery size for different depot sizes was investigated, as shown in Fig. 8. Similar to the optimization of depot size in Fig. 2, the MFSP goes through a minimum as refinery sizes are increased. For small refineries, poor economies-of-scale yield higher costs; for large refineries larger transportation costs dominate. These two forces lead to minimum MFSP at refinery sizes of 10 000–12 000 tpd. The sharp changes in the profiles are attributed to the same reasons as described for Fig. 2.

As shown in Fig. 8, an MFSP of \$3.56 per GGE (\$0.94 per GLE) is achieved for a refinery size of 10 000 tpd employing 10 depots, each having a capacity of 1000 tpd. This cost reduction with higher central refinery scale is significant for the Py-ECH system, irrespective of the comparison to the CE system.

4. Discussion

While an MFSP of \$3.62 per GGE (\$0.95 per GLE) for Py-ECH fuel is slightly lower than the \$3.71 per GGE (\$0.98 per GLE) for ethanol in the CE system, a long-term goal is to be competitive with fossil gasoline and diesel prices. In this regard,

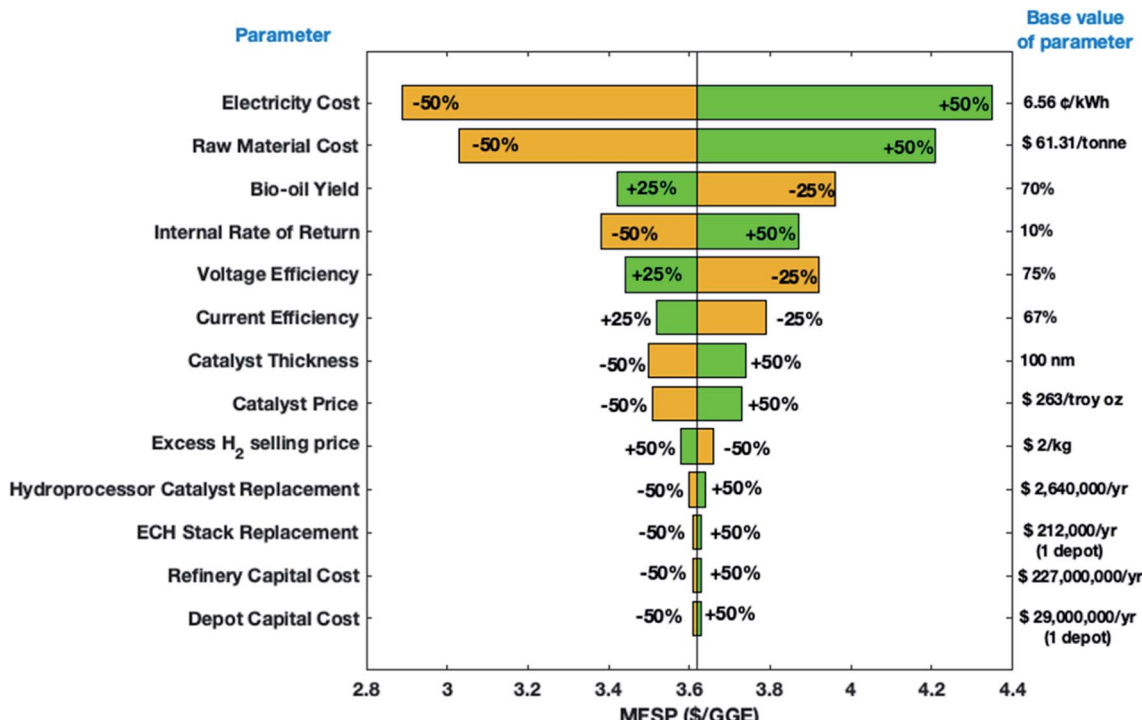


Fig. 7 Tornado plot showing MFSP single parameter sensitivity analyses for the Py-ECH-HP system (Depot size of 500 tpd and refinery size of 2000 tpd).

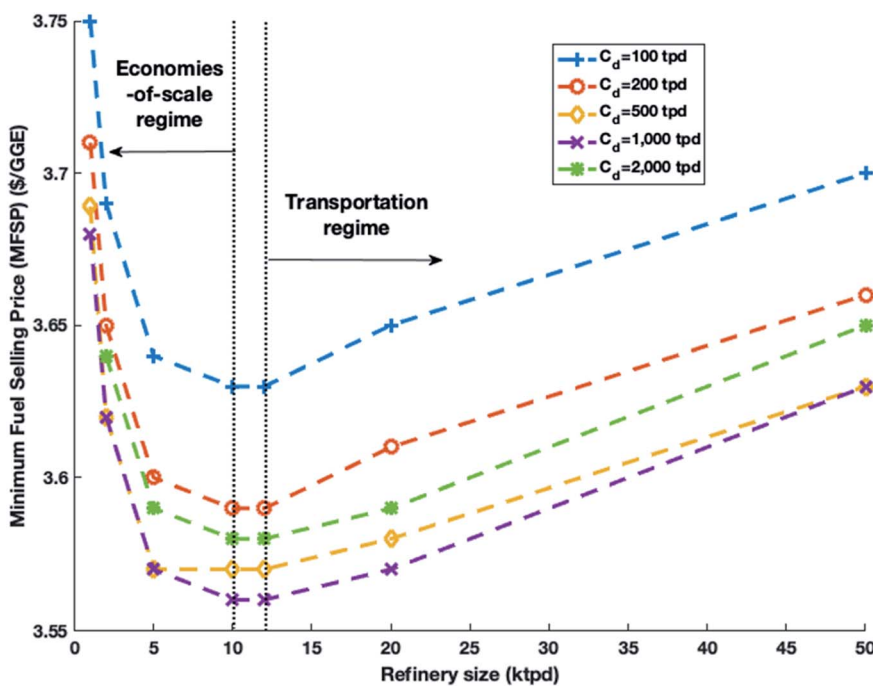


Fig. 8 MFSP versus refinery size for different depot capacities, C_d .

the sensitivity analysis (Fig. 7) points to opportunities for cost improvement: electricity cost, bio-oil yield, raw material cost, cell efficiencies, catalyst price and thickness, and the internal rate of return. However, it is difficult to improve upon the values assumed in the present model for some of these parameters.

For example, the pyrolysis bio-oil yield has been assumed at 70%, which is among the highest values in the literature. Raw material costs have already been fairly well optimized by reducing the transport costs *via* the decentralized approach in

the present model, leaving little opportunity for improvement, though waste biomass may be available at much lower price.

Utilizing low-cost electricity would be of great benefit to the Py-ECH system. While electricity has been assumed to cost \$0.066 per kW per h in the model, future costs as low as \$0.030 per kW per h are projected for wind and solar photovoltaics with advances in materials and manufacturing improvements.⁴² The U.S. Department of Energy's EIA⁴³ reports the leveledized cost of renewable electricity, without tax credits, ranging from \$0.039 per kW per h (hydroelectric) to \$0.157 per kW per h (solar thermal). The effect on MFSP of using these different electricity sources is explored in Fig. S2.† The Wind Energy Technologies Office at the U.S. Department of Energy estimates a price of \$0.010–0.020 per kW per h for electricity produced from wind sources, after applying a production tax credit. Reducing the electricity price to \$0.030 per kW per h results in a \$0.65 per GGE (\$0.17 per GLE) drop in the MFSP for Py-ECH fuel.

A current efficiency of 67% was assumed in the current model, but An *et al.* have reported current efficiencies of 70% for hydrogenation of soybean oil in a solid polymer electrolyte reactor when hydrogen is generated from electrolysis of water.⁴⁴ Pintauro *et al.* report current efficiencies as high as 97% when hydrogen gas was used for electrochemical hydrogenation of soybean oil.⁴⁵ Therefore an improvement in current efficiency from 67% to 95% may be achievable and this would lead to a further \$0.15 per GGE (\$0.04 per GLE) reduction in MFSP.

The catalyst (Ru) price, assumed at the 2019 price of \$263 per troy oz, has ranged from \$40–270 per troy oz over the last 10 years with an average of approximately \$121 per troy oz.⁴⁶ Prices rose to \$180 per troy oz in 2011, dipped to around \$40 per troy oz in 2016, then climbed to \$270 per troy oz in 2019. Using the 10 year average price of \$121 per troy oz in our calculations results in a further \$0.08 per GGE decrease in the MFSP.

Potential future improvements in voltage efficiencies and reductions in thickness of the ECH catalyst layer are difficult to estimate due to lack of information and were not considered further. As explored in the previous section, increasing the refinery size from the assumed 2000 tpd to the optimum 10 000 tpd further lowered the MFSP by \$0.06 per GGE. Finally, reducing the ECH stack replacement cost (changing replacement from 15% of installed capital costs every 7 years to 12% of installed capital costs every 10 years) yielded a very low cost reduction.⁴⁷ The final MFSP after stacking all the improvements is \$2.67 per GGE (\$0.71 per GLE) and is shown in the green bar at the extreme right in Fig. 9.

A further reduction in MFSP may be achieved by selling the by-product biochar generated at the depot. This was not considered in the base case analysis as information is lacking about the produced biochar quality and uncertainty about the price that could be obtained. Therefore, it is handled as an alternative scenario, represented by the grey bar on the right which assumes biochar can be sold at \$78.26 per tonne (the most conservative literature value found),³⁷ further reducing the final MFSP of the Py-ECH fuel to \$2.57 per GGE (\$0.68 per GLE).

The reductions in MFSP gained by stacking these improvements are shown in Fig. 9. Fig. 9 also highlights the benefit of optimizing the transportation costs in the decentralized Py-ECH system, as shown by the yellow bar on the extreme left. The unoptimized transportation cost leads to a feedstock cost of \$68.33 per dry tonne (as assumed in the CE system by Humbird *et al.*), which results in an MFSP of \$3.76 per GGE (\$0.99 per GLE). Optimization of transportation costs reduces the MFSP by \$0.14 per GGE (\$0.037 per GLE).

Our technoeconomic analysis for the Py-ECH system (where four 500 tonne per day depots process corn stover and supply ECH-stabilized bio-oil to a central refinery for further hydroprocessing) yields a projected MFSP of \$3.62 per GGE

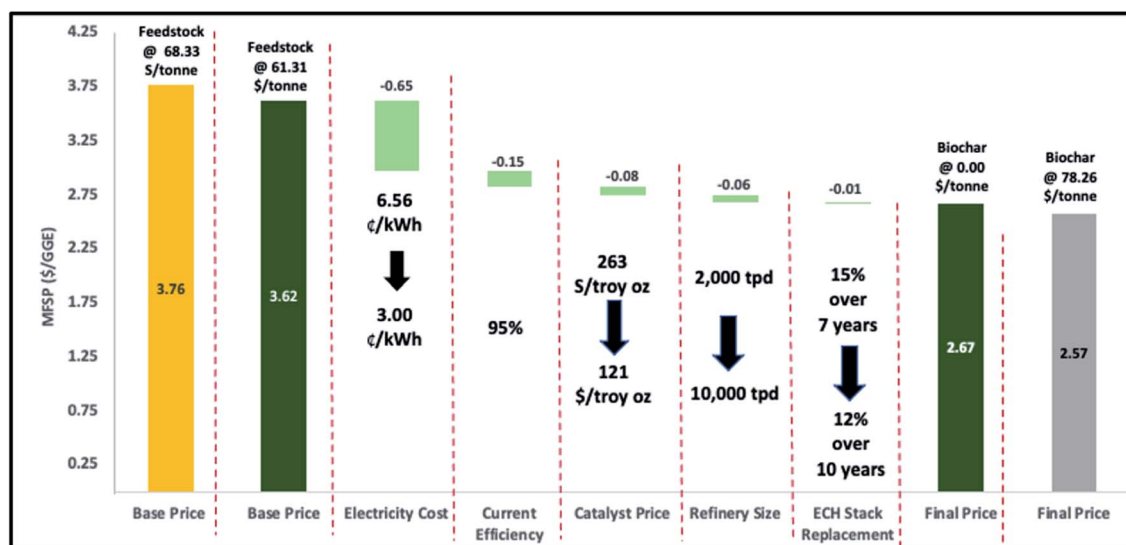


Fig. 9 Waterfall chart showing potential reduction in MFSP assuming combinations of improvements in model parameters. The light green bars show MFSP reductions from "stacking" of system improvements. The dark green bars show initial and final MFSP (after all improvements). The yellow bar at the extreme left shows the scenario when the biomass supply chain is not optimized. The grey bar at the extreme right shows the scenario when biochar is sold as a by-product.

(\$0.96 per GLE) for the final hydrocarbon fuel component. This MFSP is slightly lower than ethanol from cellulosic ethanol refineries (\$3.71 per GGE or \$0.98 per GLE) using consistent assumptions. Pathways for further reductions in MFSP were determined by varying key parameters in a sensitivity analysis. Sensitive parameters were electricity cost, raw material costs, pyrolysis bio-oil yield, ECH current efficiencies, and the price and thickness of the ECH catalyst. Stacking feasible improvements can reduce the MFSP to \$2.67 per GGE (\$0.71 per GLE), which is further reduced to \$2.57 per GGE (\$0.68 per GLE) if the by-product biochar is sold at approximately \$80 per tonne.

We have shown previously that compared to microbial bioconversion, the Py-ECH process enables significantly higher yields of renewable hydrocarbon fuels and offers a large-scale mechanism for chemical storage of renewable but intermittently generated electrical energy as transportation fuel.¹ Here we estimate MFSPs of Py-ECH renewable hydrocarbon fuels in the range of \$2.7–3.7 per GGE (\$0.71–0.98 per GLE). This range is easily competitive with the MFSPs of hydrocarbon fuels found in the literature, generated from centralized upgrading of pyrolysis bio-oils *via* hydrogen addition. Sorunmu *et al.*,²⁹ in their 2019 review, estimates this range as \$2.17–7.24 per GGE (\$0.54–0.80 per GLE). Decentralized pyrolysis and partial upgrading of biomass results in MFSPs towards the lower end of the range. One of the lowest MFSPs, \$2.34 per GGE (\$0.62 per GLE), assumes a feedstock cost of \$58 per dry ton with 50% moisture, which amounts to \$33 per tonne of biomass, compared to \$61 per tonne that is assumed in this analysis. In fact, the MFSP estimated here would be competitive to fossil gasoline and diesel prices at the higher end of their historic range of approximately \$1–4 per GGE (\$0.26–1.06 per GLE). If alternatives are successful, it would be expected that fossil gasoline and diesel prices would be driven to the lower end of their historical range. With the system described in the present study, Py-ECH renewable hydrocarbon fuels produced using renewable electricity have at least 90% lower lifecycle CO₂ emissions than gasoline, as documented in a life cycle analysis that is currently under review. In this regard, a carbon abatement subsidy or CO₂ production cost²⁹ would reduce the gap between decentralized biofuel and fossil gasoline/diesel prices. These incentives for producing fuels with lesser GHG emissions may be combined with other subsidies, including those for certain feedstocks, output-based incentives and capital grants to further lower biofuel MFSPs.⁴⁸ Future studies that incorporate carbon policies and incentives would be complementary to the present technoeconomic analysis.

Conflicts of interest

There are no conflicts to declare.

Acknowledgements

This work was funded in part by the Ford Motor Company and the National Science Foundation under award number 2055068. Dr Saffron's contribution was supported in part by the USDA

National Institute of Food and Agriculture, Hatch project 1018335, and Michigan State University AgBioResearch.

References

- 1 A. V. Bridgwater, *Fast Pyrolysis of Biomass: A Handbook*, Vol. 2, CPL Press, 2008.
- 2 A. Bridgwater, D. Meier and D. Radlein, *Org. Geochem.*, 1999, **30**, 1479–1493.
- 3 A. V. Bridgwater, *Biomass Bioenergy*, 2012, **38**, 68–94.
- 4 P. L. Eranki, B. D. Bals and B. E. Dale, *Biofuels, Bioprod. Biorefin.*, 2011, **5**, 621–630.
- 5 E. Furimsky, *Appl. Catal., A*, 2000, **199**, 147–190.
- 6 V. N. Bui, D. Laurenti, P. Afanasiev and C. Geantet, *Appl. Catal., B*, 2011, **101**, 239–245.
- 7 R. C. Baliban, J. A. Elia and C. A. Floudas, *Energy Environ. Sci.*, 2013, **6**, 267–287.
- 8 R. Rinaldi and F. Schüth, *Energy Environ. Sci.*, 2009, **2**, 610–626.
- 9 J. C. Serrano-Ruiz and J. A. Dumesic, *Energy Environ. Sci.*, 2011, **4**, 83–99.
- 10 C. Zhao, Y. Kou, A. A. Lemonidou, X. Li and J. A. Lercher, *Angew. Chem.*, 2009, **121**, 4047–4050.
- 11 T. Choudhary and C. Phillips, *Appl. Catal., A*, 2011, **397**, 1–12.
- 12 D. C. Elliott and T. R. Hart, *Energy Fuels*, 2008, **23**, 631–637.
- 13 J. Wildschut, F. H. Mahfud, R. H. Venderbosch and H. J. Heeres, *Ind. Eng. Chem. Res.*, 2009, **48**, 10324–10334.
- 14 D. A. Ruddy, J. A. Schaidle, J. R. Ferrell III, J. Wang, L. Moens and J. E. Hensley, *Green Chem.*, 2014, **16**, 454–490.
- 15 M. Saidi, F. Samimi, D. Karimipourfard, T. Nimmanwudipong, B. C. Gates and M. R. Rahimpour, *Energy Environ. Sci.*, 2014, **7**, 103–129.
- 16 S. Czernik and A. Bridgwater, *Energy Fuels*, 2004, **18**, 590–598.
- 17 Z. Li, M. Garedew, C. H. Lam, J. E. Jackson, D. J. Miller and C. M. Saffron, *Green Chem.*, 2012, **14**, 2540–2549.
- 18 Z. Li, S. Kelkar, L. Raycraft, M. Garedew, J. E. Jackson, D. J. Miller and C. M. Saffron, *Green Chem.*, 2014, **16**, 844–852.
- 19 C. H. Lam, C. B. Lowe, Z. Li, K. N. Longe, J. T. Rayburn, M. A. Caldwell, C. E. Houdek, J. B. Maguire, C. M. Saffron, D. J. Miller and J. E. Jackson, *Green Chem.*, 2015, **17**, 601–609.
- 20 M. Garedew, D. Young-Farhat, S. Bhatia, P. Hao, J. E. Jackson and C. M. Saffron, *Sustainable Energy Fuels*, 2020, **4**, 1340–1350.
- 21 M. Garedew, D. Young-Farhat, J. E. Jackson and C. M. Saffron, *ACS Sustainable Chem. Eng.*, 2019, **7**, 8375–8386.
- 22 Y. Zhou, G. E. Klinger, E. L. Hegg, C. M. Saffron and J. E. Jackson, *J. Am. Chem. Soc.*, 2020, **142**(8), 4037–4050.
- 23 M. Garedew, C. H. Lam, L. Petitjean, S. Huang, B. Song, F. Lin, J. E. Jackson, C. M. Saffron and P. Anastas, *Green Chem.*, 2021, **23**, 2868–2899.
- 24 M. M. Wright, D. E. Daugaard, J. A. Satrio and R. C. Brown, *Fuel*, 2010, **89**, S2–S10.
- 25 T. R. Brown, R. Thilakaratne, R. C. Brown and G. Hu, *Fuel*, 2013, **106**, 463–469.

26 S. B. Jones, C. Valkenburt, C. W. Walton, D. C. Elliott, J. E. Holladay, D. J. Stevens, C. Kinchin and S. Czernik, *Production of Gasoline and Diesel from Biomass via Fast Pyrolysis, Hydrotreating and Hydrocracking: a Design Case*, Pacific Northwest National Lab.(PNNL), Richland, WA (United States), 2009.

27 A. Dutta, A. Sahir, E. Tan, D. Humbird, L. J. Snowden-Swan, P. Meyer, J. Ross, D. Sexton, R. Yap and J. Lukas, *Process Design and Economics for the Conversion of Lignocellulosic Biomass to Hydrocarbon Fuels, Report NREL/TP-5100-62455, PNNL-23823*, NREL, PNNL, 2015.

28 J. L. Carrasco, S. Gunukula, A. A. Boateng, C. A. Mullen, W. J. DeSisto and M. C. Wheeler, *Fuel*, 2017, **193**, 477–484.

29 Y. Sorunmu, P. Billen and S. Spatari, *GCB Bioenergy*, 2020, **12**, 4–18.

30 M. J. Orella, S. M. Brown, M. E. Leonard, Y. Román-Leshkov and F. R. Brushett, *Energy Technol.*, 2020, **8**(11), 1900994.

31 C. H. Lam, S. Das, N. C. Erickson, C. D. Hyzer, M. Garedew, J. E. Anderson, T. J. Wallington, M. A. Tamor, J. E. Jackson and C. M. Saffron, *Sustainable Energy Fuels*, 2017, **1**, 258–266.

32 A. S. A. Dutta, E. Tan, D. Humbird, L. J. Snowden-Swan, P. Meyer, J. Ross, D. Sexton, R. Yap and J. Lukas, *Process Design and Economics for the Conversion of Lignocellulosic Biomass to Hydrocarbon Fuels, Report NREL/TP-5100-62455, PNNL-23823*, NREL, PNNL, 2015.

33 D. Humbird, R. Davis, L. Tao, C. Kinchin, D. Hsu, A. Aden, P. Schoen, J. Lukas, B. Olthof and M. Worley, *Process Design and Economics for Biochemical Conversion of Lignocellulosic Biomass to Ethanol: Dilute-Acid Pretreatment and Enzymatic Hydrolysis of Corn Stover, Report NREL/TP-5100-47764*, National Renewable Energy Laboratory (NREL), Golden, CO., 2011.

34 P. Lamers, M. S. Roni, J. S. Tumuluru, J. J. Jacobson, K. G. Cafferty, J. K. Hansen, K. Kenney, F. Teymour and B. Bals, *Bioresour. Technol.*, 2015, **194**, 205–213.

35 DOE Technical Targets for Hydrogen Production from Electrolysis, <https://www.energy.gov/eere/fuelcells/doe-technical-targets-hydrogen-production-electrolysis#:~:text=The%202020%20target%20is%20based,year%20is%20set%20to%202025.>, 2020.

36 A. Ouammi, C. Bersani, R. Sacile and H. Dagdougui, *Hydrogen Infrastructure for Energy Applications: Production, Storage, Distribution and Safety*, Elsevier Academic Press, 2018.

37 R. M. Campbell, N. M. Anderson, D. E. Daugaard and H. T. Naughton, *Appl. Energy*, 2018, **230**, 330–343.

38 M. Peters and K. Timmerhaus, *Plant Design and Economics for Chemical Engineers*, McGraw Hill, New York, 1980.

39 S. Kim and B. E. Dale, *Biomass Bioenergy*, 2015, **74**, 135–147.

40 S. Sokhansanj, S. Mani, A. Turhollow, A. Kumar, D. Bransby, L. Lynd and M. Laser, *Biofuels, Bioprod. Biorefin.*, 2009, **3**, 124–141.

41 A. Hooper and D. Murray, *An Analysis of the Operational Costs of Trucking: 2018 Update*, 2018.

42 M. J. Orella, Y. Román-Leshkov and F. R. Brushett, *Curr. Opin. Chem. Eng.*, 2018, **20**, 159–167.

43 *Levelized Cost and Levelized Avoided Cost of New Generation Resources in the Annual Energy Outlook 2019*, United States Energy Information Administration, 2019, https://www.eia.gov/outlooks/aoe/pdf/electricity_generation.pdf.

44 W. An, J. Hong and P. Pintauro, *J. Appl. Electrochem.*, 1998, **28**, 947–954.

45 P. N. Pintauro, M. P. Gil, K. Warner, G. List and W. Neff, *Ind. Eng. Chem. Res.*, 2005, **44**, 6188–6195.

46 Ruthenium Price Chart, <http://www.platinum.matthey.com/prices/price-charts#>.

47 D. Peterson, J. Vickers and D. DeSantis, *Hydrogen Production Cost from PEM Electrolysis - 2019*, 2020.

48 Z. J. Wang, M. D. Staples, W. E. Tyner, X. Zhao, R. Malina, H. Olcay, F. Allroggen and S. R. H. Barrett, *Front. Energy Res.*, 2021, **9**(9), 751722.